CrystEngComm

COMMUNICATION

View Article Online
View Journal | View Issue

Cite this: *CrystEngComm*, 2017, **19**, 4157

Received 14th January 2017,
Accepted 14th March 2017

DOI: 10.1039/c7ce00100b

rsc.li/crystengcomm

Two metal–organic frameworks sharing the same basic framework show distinct interpenetration degrees and different performances in CO_2 catalytic conversion†

Pei-Zhou Li,‡[a] Xiao-Jun Wang,‡[b] Jia Liu,‡[a] Jie Liang,[a]
Jie Yi Jalyn Chen[a] and Yanli Zhao*[ac]

Two metal–organic frameworks (MOFs) with the same basic framework but different degrees of interpenetration were successfully assembled from the same tetracarboxylate ligand and Cu(II) ions in different solvents, which show remarkably different catalytic activities in CO_2 cycloaddition reactions owing to their different pore sizes.

Metal–organic frameworks (MOFs) have been frequently demonstrated as a group of highly promising functional materials owing to their intriguing architectures and high porosity as well as their wide application potential.[1,2] MOFs are typically constructed by the coordination between polytopic bridging ligands and metal ions or clusters.[1,2] So far, numerous fascinating MOF structures have been generated from judicious assemblies of diverse organic linkers and abundant inorganic nodes under various synthetic processes, and great efforts have been dedicated to investigating their applications toward gas or small molecules, including the uptake or separation of H_2,[3] CH_4 and other hydrocarbons,[4,5] as well as CO_2.[6] MOFs have also been employed as highly efficient heterogeneous catalysts or catalyst carriers in order to address the issues of homogeneous catalytic reactions in terms of product purification and catalyst recycling.[7,8]

CO_2 has been cited as the primary anthropogenic gas, which leads to an average temperature increase of the global surface and climate change.[6,8] Thus, developing new strategies to reduce CO_2 emission has become an imperative task to scientists worldwide. Taking the emitted CO_2 as an abundant carbon source, in addition to its physical capture and storage,[6] an attractive strategy to achieve the aim of a sustainable low-carbon future should be the catalytic chemical conversion of CO_2 into value-added chemicals.[8–10] Although some MOFs have been considered as effective heterogeneous catalysts in the chemical conversion and fixation of CO_2,[8] some factors such as the pore size effect of the frameworks on the reaction substrates should be well investigated during the processes of MOF-based CO_2 chemical conversion.

In the present work, two MOFs, $\{Cu_2((C_{57}H_{36}N_{12})(COO)_4)(H_2O)_2\cdot 22(DMF)\}_n$ (**1**) and $\{Cu_2((C_{57}H_{36}N_{12})(COO)_4)(H_2O)_2\cdot 7(DMF)\}_n$ (**2**) (DMF = *N*,*N*′-dimethylformamide), were successfully fabricated,[11] which share the same basic framework by incorporating the same "clicked"-tetracarboxylate ligand with unsaturated Cu sites, but have obviously different framework interpenetration degrees, *i.e.*, 2-fold interpenetration for **1** and 4-fold interpenetration for **2**. Such a unique inherent feature makes them suitable platforms for the investigation of the interpenetration-caused pore size effect on MOF-based applications. Studies showed that the two MOFs present remarkably different catalytic activities toward CO_2 cycloaddition with the same substrates, revealing that the interpenetration-caused pore size difference between the two MOFs has a large influence on the CO_2 catalytic conversion. In other words, the substrates can easily enter the MOF with larger pores and the reaction is carried out within the framework, while the same reaction only occurs on the crystal surface of the MOF having smaller pores.

Since click chemistry is usually conducted under mild conditions with high yields, it has been widely employed in the fabrication of various functional materials.[12–14] As a typical click reaction, copper(I)-catalyzed azide–alkyne cycloaddition

---

[a] *Division of Chemistry and Biological Chemistry, School of Physical and Mathematical Sciences, Nanyang Technological University, 21 Nanyang Link, 637371, Singapore. E-mail: zhaoyanli@ntu.edu.sg*
[b] *Jiangsu Key Laboratory of Green Synthetic Chemistry for Functional Materials, School of Chemistry and Chemical Engineering, Jiangsu Normal University, Xuzhou 221116, P. R. China*
[c] *School of Materials Science and Engineering, Nanyang Technological University, 50 Nanyang Avenue, 639798, Singapore*

† Electronic supplementary information (ESI) available: Detailed experimental procedures and characterization spectra, PXRD, TGA, and CCDC 1523578 and 1523579. For ESI and crystallographic data in CIF or other electronic format see DOI: 10.1039/c7ce00100b

‡ These authors contributed equally to this work.

can lead to the generation of a 1,2,3-triazole group. It has been demonstrated that the 1,2,3-triazole group possesses high affinity to CO_2 molecules.[8g,13] Thus, by using the versatile click chemistry, a nitrogen-rich tetracarboxylate ligand, 4,4′,4″,4‴-((methane-tetrayl-tetrakis(benzene-4,1-diyl)) tetrakis-(1*H*-1,2,3-tri-azole-4,1-diyl))tetrabenzoic acid (**H_4L1**), was designed and successfully synthesized (see the ESI† for more details). Studies have also shown that Cu(II) ions in MOFs usually take the form of unsaturated paddlewheel units, which not only can significantly increase the affinity toward CO_2, but also act as catalytic Lewis acid centers in the catalytic chemical conversion of CO_2.[8g,13a,c] Therefore, Cu(II) ions were selected in the construction of MOFs with **H_4L1**. Interestingly, the phenomenon of solvent-directed assembly was observed during the preparation of MOFs.[15] When the same reactants (**H_4L1** and $Cu(NO_3)_2$) reacted in different solvents, high quality blue crystals of the two kinds of MOFs (**1** and **2**) were successfully obtained after solvothermal reactions.

Crystals suitable for single-crystal X-ray diffraction were selected and structural analyses were carried out. Both **1** and **2** share the same three-dimensional (3D) porous network with a basic framework formula of $[Cu_2(\mathbf{L1})]_n$ (without considering the coordinated water molecules and isolated organic solvents, Fig. 1, S1 and S2 in the ESI†). As shown in Fig. 1b, the coordination of two neighboring Cu(II) ions with four distributed carboxylate groups from four different **L1** ligands led to the formation of typical paddlewheel Cu_2 clusters with their locations on two-fold axes in both structures.[8g,13a,c] Then, four Cu_2 clusters are bridged by the "clicked" tetracarboxylate ligand **L1**, leading to the formation of a 3D porous framework with high porosity (Fig. 1c). It should be mentioned that the central tetrakis carbon atoms of the **L1** ligand on the two-fold axes present coordinate values of 0.5000, 0.0000, and 0.1102(3) in **1** and 0.0000, 0.5000, and 0.46000(13) in **2**. For a better insight into the nature of the complicated framework, the typical paddlewheel Cu_2 cluster can be reduced to a planar tetratopic node, while the "clicked" **L1** can be simplified to a tetrahedral tetratopic node.[1] Then, the 3D porous framework can be considered as a network with a PtS-type topology as shown in Fig. 1d.[1c,13a]

Although both **1** and **2** share the same basic 3D porous network, the degree of their framework interpenetrations is totally different. In MOF **1**, 2-fold interpenetration of the basic 3D porous network was observed, while in MOF **2**, 4-fold interpenetration occurred. In MOF **1**, two basic 3D networks regularly intertwine with each other, leaving one-dimensional porous channels in diameters of ~20 Å (point to point distance without considering the atom diameter) to be alternately arranged along the *a*- and *b*-axes, while nearly no pores are left after the 4-fold closed interpenetration in MOF **2**. After removing the discrete and coordinated solvent molecules in both structures, their porosities were calculated using the PLATON/VOID program.[16] The total solvent-accessible volumes were then estimated to be 82.9% for **1** and 63.4% for **2**, and the densities of the desolvated frameworks were calculated to be 0.345 and 0.696 g cm^{-3}, respectively, further indicating that **1** possesses high porosity and **2** is a close-packed structure. The structural analyses clearly reveal that **1** and **2** share the same basic 3D porous network, but they have quite different porosities owing to the difference in the degree of their framework interpenetration.

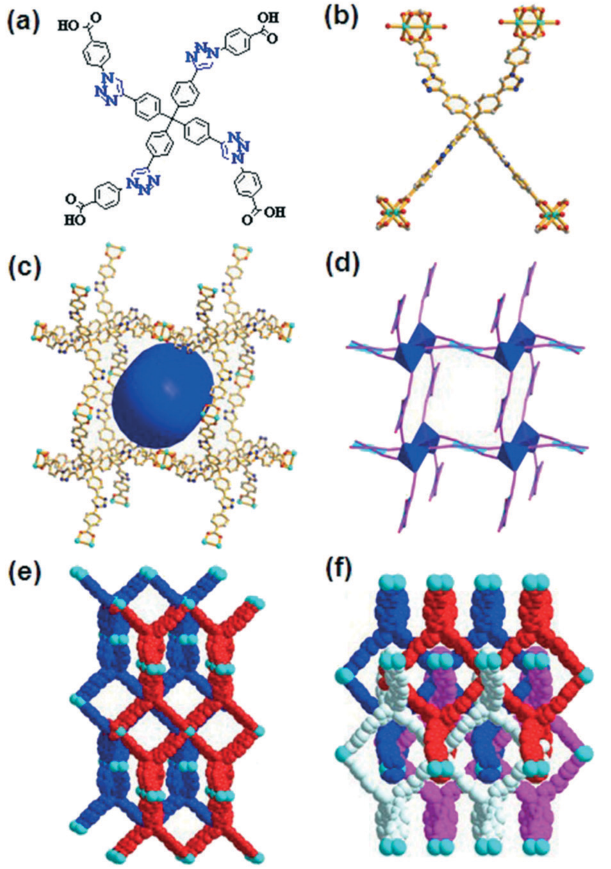

Fig. 1 (a) Schematic illustration of "click"-extended tetracarboxylate ligand **H_4L1**, (b) coordination of **L1** with paddlewheel Cu_2 units in the frameworks, (c) perspective view of the basic 3D frameworks of **1** and **2** with a large pore (blue ball) along the *c*-axis, (d) illustration of the "PtS"-type topological network of **1** and **2** showing the fascinating combination of planar tetratopic paddlewheel Cu_2 clusters and tetrahedral tetratopic **L1** linkers, (e) and (f) illustrations of 2-fold (for **1**) and 4-fold (for **2**) framework interpenetrations in crystals.

Nitrogen adsorption measurements were then carried out to confirm their porosity. The as-synthesized crystals of both MOFs were firstly activated by thoroughly exchanging the solvents with chloroform, and then degas processes were conducted under vacuum at 80 °C for 6 hours followed by gas adsorption measurements. The powder X-ray diffraction (PXRD) patterns of the activated samples present good agreement with the related PXRD patterns calculated from their crystal data (Fig. S3 and S4 in the ESI†), indicating that both frameworks were well maintained after the activation. Then, the activated samples were subjected to N_2 sorption at 77 K. As illustrated in Fig. 2a and b, MOFs **1** and **2** exhibit typical reversible type I sorption isotherms with a quickly increased step prior to the plateau, demonstrating that both of them possess a microporous feature.[17] However, the overall N_2

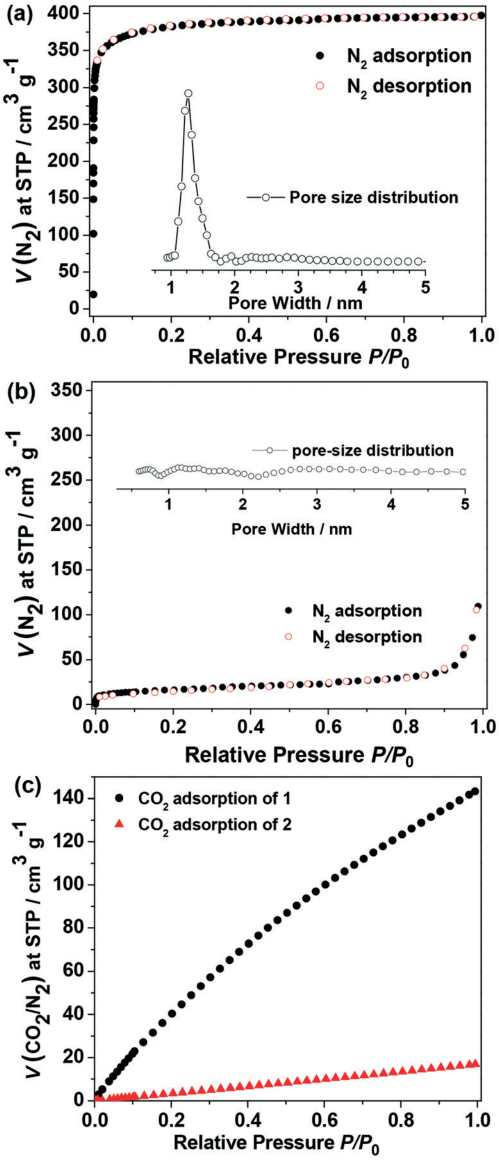

Fig. 2 N_2 adsorption/desorption isotherms and pore size distributions of (a) **1** and (b) **2** at 77 K, and (c) CO_2 adsorption isotherms of **1** and **2** at 273 K.

uptake and the calculated Brunauer–Emmett–Teller (BET) surface areas of **1** and **2** are quite different. The N_2 uptake of **1** is 397.4 cm^3 g^{-1} at 1 atm with the BET surface area calculated to be 1513 m^2 g^{-1}. The N_2 uptake of **2** is only in the range of 10–38 cm^3 g^{-1} at the plateau followed by an increase to 109.3 cm^3 g^{-1} at 1 atm, giving a BET surface area of only 58.2 m^2 g^{-1}. Their pore size distributions were also calculated based on the N_2 sorption isotherms at 77 K with non-local density functional theory, revealing that **1** possesses a pore size distribution ranging from 1.0 to 1.6 nm, while **2** shows nearly no pores. The calculated pore size distributions are well consistent with the observations from their crystal structures. Their CO_2 sorption capabilities were also measured. As shown in Fig. 2c, **1** shows a CO_2-uptake value of 143.2 cm^3 g^{-1} at 273 K and 1 atm, while **2** gives a CO_2-uptake value of only 16.9 cm^3 g^{-1} under the same conditions.

The above analyses clearly indicate that **1** and **2** have the same basic 3D porous network with the same type of catalytically active Lewis-acid Cu_2 paddlewheel centers, but different porosities caused by the different degrees of their framework interpenetration. This inherent feature makes them good platforms for the investigation of the interpenetration-caused pore size effect on MOF-based catalytic conversion of CO_2. Owing to wide applications of the produced carbonates in the pharmaceutical and electrochemical industries,[8,18] catalytic cycloaddition of CO_2 with epoxides to produce cyclic carbonates has been intensively investigated. Thus, catalytic CO_2 cycloaddition with epoxides (Scheme 1) was selected as a model reaction in our investigation of the pore-size effect on the catalytic conversion of CO_2.

Four typical liquid substrates, methyloxirane, 2-ethyloxirane, 2-(chloromethyl)oxirane, and 2-(bromomethyl)oxirane, were selected and the reactions were carried out in a Schlenk tube. In a typical reaction, 40 mmol methyloxirane and 0.16 mmol MOF catalysts (0.4 mol% based on paddlewheel units) with 1.0 g tetrabutyl ammonium bromide (TBAB) as the co-catalyst were introduced into the tube, and the mixture was stirred at room temperature under 1 atm CO_2 for 60 h. The yields of the obtained cyclic carbonates produced from CO_2 with related epoxides catalyzed by **1** and **2** were then determined. As shown in Fig. 3, the cyclic carbonate production yields catalyzed by **1** are 94% for 2-methyloxirane, 80% for 2-ethyloxirane, 83% for 2-(chloromethyl)oxirane, and 85% for 2-(bromomethyl)oxirane (Fig. S7 in the ESI†), while the production yields of cyclic carbonates produced under the same processes catalysed by **2** are only 49%, 33%, 35%, and 36%, respectively (Fig. S8 in

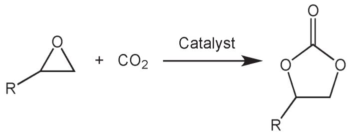

Scheme 1 Catalytic CO_2 cycloaddition with epoxides to produce cyclic carbonates.

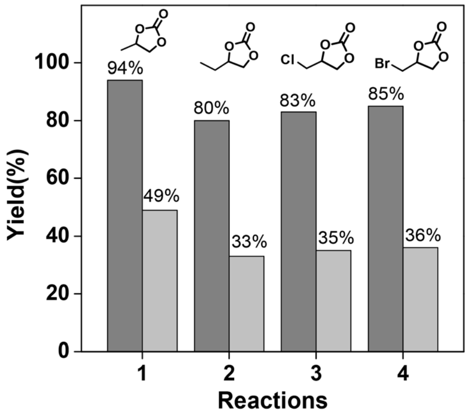

Fig. 3 Yields of cyclic carbonates produced from CO_2 cycloaddition with related epoxides catalyzed by **1** (black) and **2** (gray) under 1 atm CO_2 pressure at room temperature for 60 h.

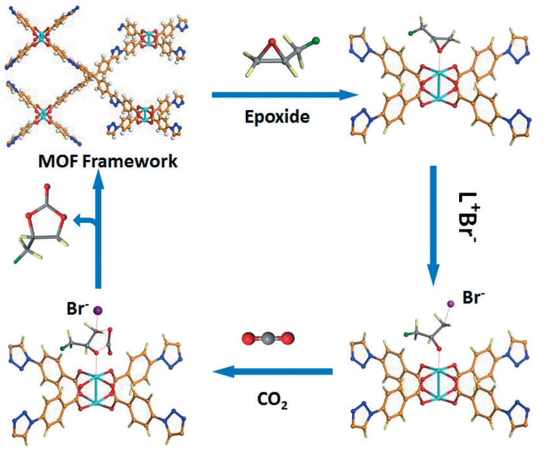

Fig. 4 Scheme of the catalytic mechanism for the reactions of epoxides and CO_2 into cyclic carbonates catalyzed by MOFs **1** and **2** (peacock blue sphere: open Cu site; L^+ = tetra-*n*-butylammonium; green sphere in epoxide: H, CH_3, Cl, or Br).

the ESI†). The comparison of the yields for all the four substrates clearly demonstrates that MOFs **1** and **2** present remarkably different catalytic activities toward CO_2 catalytic cycloaddition with the same substrates under the same reaction conditions.

The MOF-based catalytic mechanism (Fig. 4) was investigated according to previous reports.[8] The MOFs present activity for CO_2 conversion due to the exposed Lewis-acid Cu sites. As shown in Fig. 4, the unsaturated orbital of Cu in the activated framework of **1** or **2** can accept electrons from donors such as the O atom of propylene oxide. After binding with Cu, part of the electron transfer from the O atom of epoxide to Cu leads to the weakening of the C–O bond in epoxide. Subsequently, the Br^- generated from ^{t}Bu$_4$NBr attacks the less-hindered C atom of epoxide to open the epoxy ring. Then, the O atom from CO_2 attacks the positively charged C atom of epoxide together with an attack from the O atom of epoxide on the C atom of CO_2. Finally, a ring closure step leads to the production of cyclic carbonate. Given the similar basic framework with the same type of Lewis acid metal sites in both **1** and **2**, the different catalytic activities between **1** and **2** should be ascribed to the interpenetration-caused pore size difference, *i.e.*, the substrate can easily enter the MOF with larger pores and the reaction is carried out within the framework, while the same reaction only occurs on the crystal surface of the MOF with smaller pores. Thus, the studies clearly reveal that the interpenetration-caused pore size difference of the framework has a large influence on the MOF-based CO_2 catalytic conversion.

Since **1** shows much higher catalytic activity in CO_2 cycloaddition with methyloxirane, the recyclability of MOFs was tested by taking this cycloaddition as an example. The results exhibit that there was no significant decrease in catalytic activity after 5 cycles of reactions (Fig. S9 in the ESI†). The PXRD patterns of the recycled **1** are also well consistent with the calculated patterns from its crystal data (Fig. S10 in the ESI†), indicating that the framework of **1** was maintained during the catalytic reactions.

In summary, two MOFs having the same basic framework but different interpenetration degrees have been constructed *via* the assemblies of triazole-containing tetracarboxylate linkers with Cu ions in different organic solvents. The two MOFs incorporate the same tetracarboxylate ligands and unsaturated Cu sites, but present obviously different pore sizes caused by different degrees of interpenetration. Their unique inherent feature makes them suitable platforms for the study of the interpenetration-caused pore size effect on MOF-based applications. Detailed investigations have shown that the two MOFs exhibit remarkably different catalytic activities in CO_2 cycloaddition reactions with the same substrates, indicating that the interpenetration-caused pore size differences of the frameworks have a large influence on MOF-based CO_2 catalytic conversion.

This research is financially supported by the Singapore Academic Research Fund (RG112/15 and RG19/16).

Notes and references

1 (*a*) C. Janiak and J. K. Vieth, *New J. Chem.*, 2010, **34**, 2366; (*b*) M. O'Keeffe and O. M. Yaghi, *Chem. Rev.*, 2012, **112**, 675; (*c*) M. Li, D. Li, M. O'Keeffe and O. M. Yaghi, *Chem. Rev.*, 2014, **114**, 1343.

2 (*a*) H. Wu, Q. Gong, D. H. Olson and J. Li, *Chem. Rev.*, 2012, **112**, 836; (*b*) P.-Z. Li and Y. Zhao, *Chem. – Asian J.*, 2013, **8**, 1680; (*c*) Y. Zhao, *Chem. Mater.*, 2016, **28**, 8079.

3 (*a*) J. Sculley, D. Yuan and H.-C. Zhou, *Energy Environ. Sci.*, 2011, **4**, 2721; (*b*) M. P. Suh, H. J. Park, T. K. Prasad and D.-W. Lim, *Chem. Rev.*, 2012, **112**, 782.

4 (*a*) Y. He, W. Zhou, T. Yildirim and B. Chen, *Energy Environ. Sci.*, 2013, **6**, 2735; (*b*) Y. He, W. Zhou, G. Qiand and B. Chen, *Chem. Soc. Rev.*, 2014, **43**, 5657.

5 (*a*) S.-C. Xiang, Z. Zhang, C.-G. Zhao, K. Hong, X. Zhao, D.-R. Ding, M.-H. Xie, C.-D. Wu, M. C. Das, R. Gill, K. M. Thomas and B. Chen, *Nat. Commun.*, 2011, **2**, 204; (*b*) H. Wu, Q. Gong, D. H. Olson and J. Li, *Chem. Rev.*, 2012, **112**, 836.

6 (*a*) K. Sumida, D. L. Rogow, J. A. Mason, T. M. McDonald, E. D. Bloch, Z. R. Herm, T.-H. Bae and J. R. Long, *Chem. Rev.*, 2012, **112**, 724; (*b*) J. Liu, P. K. Thallapally, B. P. McGrail, D. R. Brown and J. Liu, *Chem. Soc. Rev.*, 2012, **41**, 2308.

7 (*a*) T. Zhang and W. Lin, *Chem. Soc. Rev.*, 2014, **43**, 5982; (*b*) A. H. Chughtai, N. Ahmad, H. A. Younus, A. Laypkov and F. Verpoort, *Chem. Soc. Rev.*, 2015, **44**, 6804.

8 (*a*) J. Song, Z. Zhang, S. Hu, T. Wu, T. Jiang and B. Han, *Green Chem.*, 2009, **11**, 1031; (*b*) C. M. Miralda, E. E. Macias, M. Zhu, P. Ratnasamy and M. A. Carreon, *ACS Catal.*, 2012, **2**, 180; (*c*) O. V. Zalomaeva, A. M. Chibiryaev, K. A. Kovalenko, O. A. Kholdeeva, B. S. Balzhinimaev and V. P. Fedin, *J. Catal.*, 2013, **298**, 179; (*d*) W.-Y. Gao, Y. Chen, Y. Niu, K. Williams, L. Cash, P. J. Perez, L. Wojtas, J. Cai, Y.-S. Chen and S. Ma, *Angew. Chem., Int. Ed.*, 2014, **53**, 2615; (*e*) J.

Zheng, M. Wu, F. Jiang, W. Su and M. Hong, *Chem. Sci.*, 2015, **6**, 3466; (*f*) X. Han, X.-J. Wang, P.-Z. Li, R. Zou, M. Li and Y. Zhao, *CrystEngComm*, 2015, **17**, 8596; (*g*) P.-Z. Li, X.-J. Wang, J. Liu, J. S. Lim, R. Zou and Y. Zhao, *J. Am. Chem. Soc.*, 2016, **138**, 2142.

9 (*a*) C. D. N. Gomes, O. Jacquet, C. Villiers, P. Thuery, M. Ephritikhine and T. Cantat, *Angew. Chem., Int. Ed.*, 2012, **51**, 187; (*b*) X.-B. Lu and D. J. Darensbourg, *Chem. Soc. Rev.*, 2012, **41**, 1462.

10 (*a*) K. Iizuka, T. Wato, Y. Miseki, K. Saito and A. Kudo, *J. Am. Chem. Soc.*, 2011, **133**, 20863; (*b*) Y. Xie, T.-T. Wang, X.-H. Liu, K. Zou and W.-Q. Deng, *Nat. Commun.*, 2013, **4**, 1960; (*c*) W. Tu, Y. Zhou and Z. Zou, *Adv. Mater.*, 2014, **26**, 4607; (*d*) S. Lin, C. S. Diercks, Y.-B. Zhang, N. Kornienko, E. M. Nichols, Y. Zhao, A. R. Paris, D. Kim, P. Yang, O. M. Yaghi and C. J. Chang, *Science*, 2015, **349**, 1208.

11 MOFs **1** and **2** in the main text can be cited as **NTU-140** and **NTU-141**, respectively.

12 (*a*) H. C. Kolb, M. G. Finn and K. B. Sharpless, *Angew. Chem., Int. Ed.*, 2001, **40**, 2004; (*b*) V. V. Rostovtsev, L. G. Green, V. V. Fokin and K. B. Sharpless, *Angew. Chem., Int. Ed.*, 2002, **41**, 2596.

13 (*a*) X.-J. Wang, P.-Z. Li, Y. Chen, Q. Zhang, H. Zhang, X. X. Chan, R. Ganguly, Y. Li, J. Jiang and Y. Zhao, *Sci. Rep.*, 2013, **3**, 1149; (*b*) P.-Z. Li, X.-J. Wang, K. Zhang, A. Nalaparaju, R. Zou, R. Zou, J. Jiang and Y. Zhao, *Chem. Commun.*, 2014, **50**, 4683; (*c*) P.-Z. Li, X.-J. Wang, J. Liu, J. S. Lim, R. Zou and Y. Zhao, *J. Am. Chem. Soc.*, 2016, **138**, 2142.

14 (*a*) L. Sun, Y. Li, Z. Liang, J. Yu and R. Xu, *Dalton Trans.*, 2012, **41**, 12790; (*b*) Y. Yan, M. Suyetin, E. Bichoutskaia, A. J. Blake, D. R. Allan, S. A. Barnett and M. Schroder, *Chem. Sci.*, 2013, **4**, 1731; (*c*) H. Xu, J. Gao and D. Jiang, *Nat. Chem.*, 2015, **7**, 905.

15 (*a*) P.-Z. Li, X.-J. Wang, Y. Li, Q. Zhang, R. H. D. Tan, W. Q. Lim, R. Ganguly and Y. Zhao, *Microporous Mesoporous Mater.*, 2013, **176**, 194; (*b*) F. Sun and G. Zhu, *Inorg. Chem. Commun.*, 2013, **38**, 115; (*c*) X.-M. Jing, L.-W. Xiao, L. Wei, F.-C. Dai and L.-L. Ren, *Inorg. Chem. Commun.*, 2016, **71**, 78.

16 A. Spek, *Acta Crystallogr., Sect. D: Biol. Crystallogr.*, 2009, **65**, 148.

17 K. S. W. Sing, D. H. Everett, R. A. W. Haul, L. Moscou, P. A. Pierotti, J. Rouquerol and T. Siemieniewska, *Pure Appl. Chem.*, 1985, **57**, 603.

18 M. North, R. Pasquale and C. Young, *Green Chem.*, 2010, **12**, 1514.